Time-Resolved Fluorescence of Salicylideneaniline Compounds in Solution

Víctor Vargas C.*

Laboratory of Luminescence and Molecular Structure, Department of Chemistry, Faculty of Sciences, University of Chile, Casilla 653, Santiago, Chile

Received: May 27, 2003; In Final Form: October 31, 2003

The substituent effect on the dynamics of deactivation of the first singlet excited state of para-substituted salicylideneaniline in octanol was investigated using multifrequency phase and modulation fluorometry. On the basis of the temperature dependence and by use of the global analysis approach to the excited-state reaction scheme, we have determined the rate and the activation energy for the *cis*-keto* → *twist*-keto* process. It has been found that the activation energy increases when the electron-donor strength of the substituent increases.

Introduction

Intramolecular proton-transfer reactions in solid phase or in solution are of great interest from both the basic[1−6] and applied[7−9] viewpoints. Molecules with adjacent acidic and basic functional groups are able to undergo intermolecular proton transfer. In many cases, the proton affinities of these sites change upon photoexcitation, leading to excited-state intramolecular proton transfer (ESIPT).

Salicylideaniline and related molecules display ESIPT. The study of the tautomeric equilibrium of these systems has been the subject of considerable interest, from both experimental[10−21] and theoretical points of view.[15,17,18−23] The scope of these studies was to obtain insight about the principal factors and mechanisms that modulate the ESIPT process. In these studies, a kinetic model for the deactivation of the first excited state was proposed. These studies make use of time-resolved fluorescence techniques in the pico- or femtosecond time scales.

In a previous paper,[17] we have reported a study of the enol-imine ↔ keto-amine tautomeric equilibrium in the ground electronic state of the *N*-salicylidene-*p*-X-aniline compounds. We analyzed the para-substitution effect on the tautomeric equilibrium constants $K°_{tau}$ and standard thermodynamics properties. In this paper, we perform a photophysical study on the salicylideaniline compounds **1**−**6** shown in Figure 1. The aim of this paper is to analyze, from an experimental and theoretical viewpoint, the effect promoted by electron-donor and electron-acceptor substitution at the phenylaniline ring on the kinetics of the deactivation of the first singlet excited state. We also propose a model for the excited-state reaction of the two keto tautomeric species. The lifetime data of these *N*-salicylidene-*p*-X-aniline compounds in solution were obtained by using the multifrequency phase and modulation techniques.[24] The rate and the activation energy for this isomeric excited-state reaction are calculated from lifetime measurements in octanol as a function of the temperature by using the global analysis procedure.[25] Furthermore, we analyzed experimentally and theoretically the effect of the para substitution at the phenylaniline ring of *N*-salicylidene-aniline compounds on the rate and on the activation energies for the intramolecular rotation process in the first excited state.

To obtain more insights about the excited-state isomeric process, we performed ab initio molecular orbital calculations for the *cis*-keto* → *trans*-keto* transition.

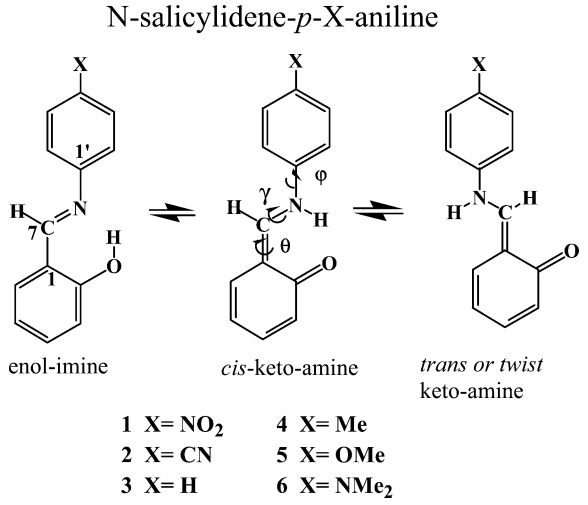

Figure 1. *N*-Salicylidene-*p*-X-aniline series and conformational isomers. θ and φ represent keto (K) and aniline (A) ring rotation, respectively.

Experimental and Computational Methods

N-Salicylidene-*p*-X-aniline compounds, with X = Me, OMe, NMe_2 as electron-donor substituents and X = NO_2, CN as electron-acceptor substituents, were synthesized by a condensation procedure stirring equimolar quantities of salicylaldhehyde and aniline in methanol solution. Double crystallizations were carried out in methanol at low temperature followed by vacuum sublimation. The structure of the compounds under study was determined from IR and ^{1}H NMR data. Solutes and solvents, cyclohexane, ethanol, butanol, and octanol from Aldrich, were HPLC grade, with very low fluorescence background.

Absorption spectra were recorded in a Perkin-Elmer Lambda 11 UV−vis spectrophotometer in a 10-mm quartz cell. The fluorescence spectra were recorded in the ISS-PC photon-counting spectrofluorometer, which is coupled to a thermoregulated methanol bath. The quantum yields of fluorescence were measured by comparison with quinine bisulfate ($\phi_f = 0.51$) in 0.05 M H_2SO_4.

Time-resolved measurements were performed by using an ISS Greg-200 multifrequency phase and modulation fluorometer.

* Phone: 56-2-678 7341. Fax: 56-2-271 3888. E-mail: victor@uchile.cl.

10.1021/jp035461w CCC: $27.50
Published on Web 12/13/2003

Excitation was accomplished using a cavity-dumped Rhodamine dye laser system synchronously pumped by a mode-locked Nd−Yag laser (Coherent Antares). The rhodamine dye laser was frequency doubled to generate excitation at 345 nm. The emission was observed through a Schott KV 450-nm cut-on filter. The exciting light was polarized at an angle of 33° with respect to the vertical direction to eliminate polarization effects in the lifetime values. The modulation frequency was in the range of 30−400 MHz.

In the multifrequency phase and modulation technique, the excitation light intensity is modulated. The phase shift and the relative modulation of emission and lifetime are calculated according to eq 1

$$\tan(P) = \omega\tau^p$$

$$M = [1 + (\omega\tau^M)^2]^{-1/2} \qquad (1)$$

where P is the phase shift, M the relative modulation, and ω the angular frequency of the excitation light.

The measured-phase and the modulation values are analyzed as a sum of exponentials

$$I(t) = \sum_i^n f_i \, e^{-t/\tau_i}$$

with

$$\sum_i^n f_i = 1 \qquad (2)$$

f_i is the fractional contribution to the total fluorescence intensity. In the nonlinear least-squares approach, the goodness of fit of measured-phase and modulation data to a particular model (e.g., single or double exponential) is judged by the values of reduced chi squared (χ^2) as defined by eq 3

$$\chi^2 = \frac{\sum_1^n \left\{ \left(\frac{P_c - P_m}{\sigma^P} \right)^2 + \left(\frac{M_c - M_m}{\sigma^M} \right)^2 \right\}}{(2n - f - 1)} \qquad (3)$$

The sum is performed over all the measurements at n modulation frequency, and f is the number of free parameters. P and M correspond to the phase-shift and the relative modulation values, respectively. Indexes c and m indicate the calculated and measured values, respectively. σ^P and σ^M correspond to the standard deviations of each phase and the modulation measurements, respectively. The analysis was accomplished by means of the Globals Unlimited Software.[26] The σ^P and σ^M values were 0.2° and 0.004, respectively.

The enol and keto structures were optimized by means of ab initio calculations using the Gaussian 98 software at the restricted Hartree−Fock level using the standard 6-31G basis set. In the first excited-state calculation, we have used a partial configuration interaction (CIS) and the active-space multiconfiguration including 11 HOMO and 11 LUMO states.

Results and Discussion

(a) Absorption and Fluorescence Spectra. Figure 2 displays the absorption and fluorescence spectra of the **4** (X = Me) and **6** (X = NMe_2) compounds in ethanol solution at 293−295 K. The spectra of the other compounds exhibit similar characteristics to those shown in Figure 2. The absorption spectra of the

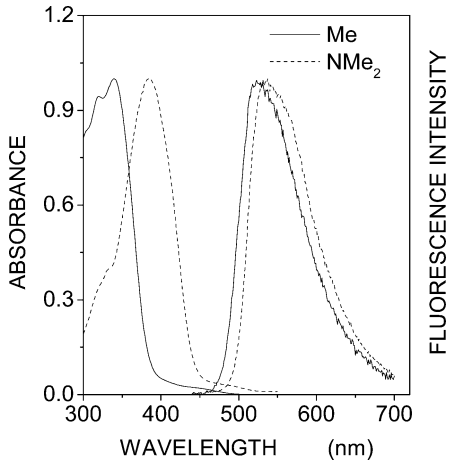

Figure 2. Absorption and fluorescence spectra of methyl- and dimethylamine-substituted compounds in ethanol solution.

TABLE 1: Frequency of Absorption and Fluorescence Maximum (ν_{ab}, ν_{em}), Stokes Shift ($\nu_{ab} - \nu_{em}$), and Fluorescence Quantum Yields (ϕ_f)[a] of *N*-salicilydene-*p*-X-aniline Compounds in Solutions at 22 °C

solvent	substituent	ν_{ab} (cm^{-1})	ν_{em} (cm^{-1})	$\nu_{ab} - \nu_{em}$ (cm^{-1})	ϕ_f 10^4
CHEX	NO_2	28010	18120	9890	1.6
	CN	28410	18430	9980	1.1
	H	29200	18550	10650	0.7
	Me	28900	18910	9990	1.1
	OMe	28330	18990	9340	1.6
	NMe_2	26010	18950	7060	15.0
ETOH	NO_2	27790	17620	10170	1.4
	CN	29050	17860	11190	1.6
	H	29500	19050	10450	2.1
	Me	29330	19160	10170	2.7
	OMe	28510	19170	9340	4.9
	NMe_2	26160	18930	7250	12.4
BUTOH	NO_2	27590	17980	9610	2.3
	CN	28490	18420	10070	3.5
	H	29410	18790	10620	2.3
	Me	29070	18990	10080	3.3
	OMe	28530	19060	9470	5.3
	NMe_2	25840	18780	7060	17.1
OCTOH	NO_2	27800	18100	9700	3.9
	CN	28310	17910	10400	4.9
	H	29090	18620	10440	5.0
	Me	28840	18790	10050	6.3
	OMe	28380	19230	9150	12.4
	NMe_2	25640	18950	6690	53.3

[a] Respect to quinine sulfate in sulfuric acid 0.1 N, $\phi = 0.54$.

N-salicylidene-*p*-X-aniline compounds are characterized by a broad and intense band at 340 nm. A bathochromical shift is observed according to the electron-acceptor or electron-donor strength of the substituents. In the hydroxylic solvents, we observe in the 430−500-nm region a new weak absorption band, which is associated with the keto isomer.[17,23]

The fluorescence spectra of compounds **1**−**6** are characterized by a weak emission band in the 520−540-nm region (Figure 2). These spectra display a large batochromical shift with respect to the absorption spectra (Stokes shift). The origin of this emission has been previously attributed to excited keto tautomer species[1−3,11,13] generated by a very fast enol-imine* → *cis*-keto-amine* ESIPT.

In Table 1, we display the frequency (cm^{-1}) of the absorption and fluorescence bands maxima of compounds **1**−**6** dissolved in cyclohexane and hydroxilic solvent. In this table, it is possible to observe that the absorption maximum is redshifted by about 3000 cm^{-1} by increasing the donor strength of the substituent

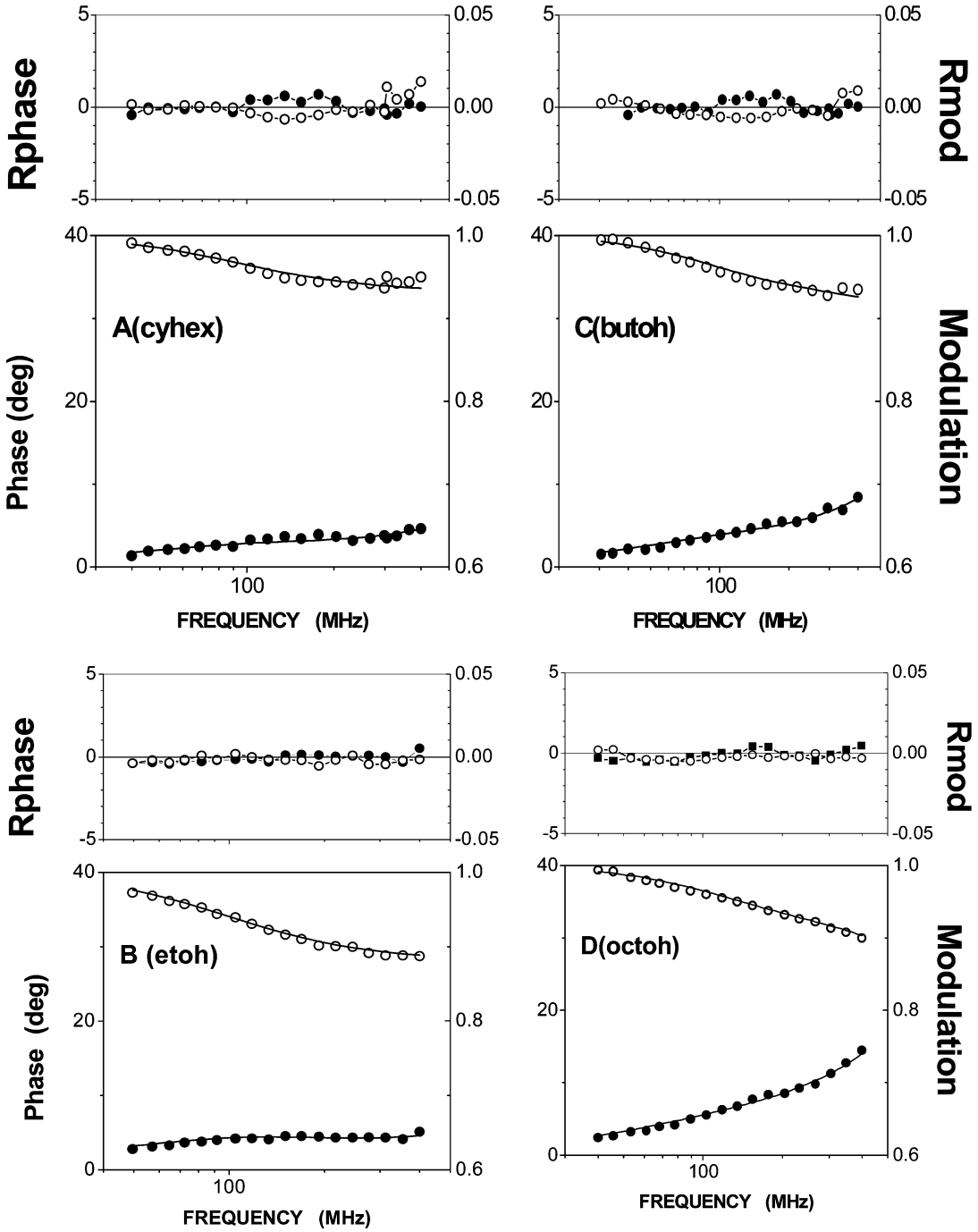

Figure 3. Phase (●) and modulation (○) lifetime data of salicylideneaniline in solution. (A) cyclohexane, (B) ethanol, (C) butanol, and (D) octanol. The solid line corresponds to the better fit with two-exponential component models. The Rphase and Rmod are the residues based on the fit to the indicated decay scheme.

(compounds **3**−**6**). On the other hand, the frequency of the fluorescence maxima shows a moderate hipsochromical shift upon increasing the electron-donor strength of the substituent (except compound **6**). The Stokes shift goes from 10 000 cm^{-1} in nitro to 7000 cm^{-1} in dimethylamine-substituted compounds.

Fluorescence quantum yields are displayed in Table 1. Chemical substitution, in all solvents, produces an increase in the fluorescence intensity by increasing the electron-donor properties of the substituent. The origin of this enhancement could be attributed to the stabilization of the lowest singlet state (π,π^*) when increasing the electron-donor properties of the substituent. The solvent effect on the fluorescence quantum yield shows an intensity increase by a factor of 2.7 (average) in octanol when compared to ethanol solvent. The solvent polarity change is too small to explain the observed intensity changes, and our explanation requires the consideration of the kinetics of deactivation of the first excited state.

(b) Time-Resolved Results. In previous time-resolved studies of the salicylideaniline compounds, time-domain techniques with pico- or femtosecond resolution were used.[11,13−15,18] These techniques assessed well the information about the photo process rates smaller than 1 ps^{-1}. For salicylideneaniline in ethanol solution, the proton-transfer rate is about 0.2 ps^{-1} [11] and 4.7 and 2.6 ps^{-1} in cyclohexane and ethanol, respectively.[14] For the sacilydene-*p*-methylaniline, a value of 0.3 ps^{-1} in the crystalline phase was reported.[13]

In our time-resolved study, we used frequency-domain techniques in the 30−400 MHz range. To our knowledge, there

is no lifetime data reported on salicylideneaniline compounds measured using the frequency-domain technique. This technique will allow us to simultaneously measure with high accuracy the short- and long-lifetime components of the decay. By use of this technique at 400 MHz and eq 1, we obtain for a 5 ps process values of the phase shift and modulation equal to $\phi = 0.720 \pm 0.2$ and $M = 0.999 \pm 0.004$, respectively. Therefore, in accordance with our experimental uncertainties, in the 30−400 MHz range, we can only quantify those processes taking place after the enol* → keto* excited-proton transfer.

The multifrequency phase and the modulation data of the salicylidenaniline in cyclohexane and alcoholic solutions are shown in Figure 3. The best fit is achieved (low reduced χ^2 values, eq 3) with two exponential components. We have found, for salicylidenaniline in ethanol at 293 K, $\tau_1 = 0.020 \pm 0.002$ ns, $f_1 = 0.89$, $\tau_2 = 1.76 \pm 0.1$ ns, and $f_2 = 0.11$ for the lifetime τ and intensity fraction, respectively.

Our lifetime values are in agreement with $\tau = 0.020 \pm 0.002$ ns found by Barbara et al.[11] They recovered, by using time-domain techniques, only one component. At low temperature (4 K), they recovered a second component of 3 ns at a longer wavelength. Recently, Mitra and Tamai[14] reported the fluorescence decay analysis of a salicylidenaniline compound in cyclohexane and ethanol solvents in the emission maximum (540 nm). The experimental resolution of their systems is 30 ps (fwhm). The fluorescence decay data were analyzed using a sum of two exponentials. Interestingly, the pre-exponential factor associated with the long decay was less than 0.1%. The fluorescence lifetimes were ≈4 ps in cyclohexane and ≈11 ps in ethanol. However, they do not report values for the long lifetime component.

Figure 3 shows that in cyclohexane (A) and ethanol (B) solution, the phase-shift and the modulation data are very similar. However, above 100 MHz, when the aliphatic alcohol chain length increases (parts B, C, and D of Figure 3), we note that the phase-shift plots are different. These results are discussed later along with data for other *N*-salicylideneaniline compounds in connection with the proposed decay model.

In Table 2, we report results for the two-exponential decay of the salicylidene compounds (**1**−**6**) in cyclohexane and alcoholic solutions. In cyclohexane solution, all compounds show that both lifetime components are similar. Thus, the short-lifetime component, τ_S, is about 0.02 ns (except compound 6) and the long-lifetime component, τ_L, is about 1.5 ns. These lifetimes correlate well with the electronic nature of the substitution. In alcoholic solution we observe that (a) the short-lifetime component increases with increasing the electron-donor strength from nitro- to dimethylamine-substituted compounds and (b) in all compounds the shorter-lifetime component increases with the chain length of the aliphatic alcohol. Therefore, we find that in butanol and octanol the short-lifetime component increases on average 2.2 and 3.9 times with respect to the lifetime in ethanol. We also note that the intensity fraction of this component increases with the polarity of the solvent. These variations of the short-lifetime component cannot be assigned solely to the solvent polarity effect since the observed spectral shifts are small. (See Table 1.)

The solvent viscosities are 1.2 (ethanol), 2.9 (butanol), and 10.0 cp (octanol). This solvent property plays an important role in the modulation of the deactivation dynamics of the first excited state of the salicylidenaniline compounds.

(c) Temperature and Viscosity Effect. In Figure 4, we show the lifetime and the fraction of compound 3 in octanol at different temperatures in the 267−325 K range. We note that

TABLE 2: Two-Component Lifetimes and Fractional Intensities of *N*-Salicilydene-*p*-X-aniline Compounds in Solutions at 22 °C[a]

solvent	substituent	τ_S	f_S	τ_L	f_L	χ^2
CHEX	NO_2	0.029	0.917	1.450	0.083	1.7
	CN	0.017	0.915	1.357	0.085	1.9
	H	0.026	0.934	1.751	0.066	2.3
	Me	0.020	0.930	1.592	0.070	2.0
	OMe	0.028	0.936	1.605	0.064	1.7
	NMe_2	0.069	0.938	1.476	0.062	1.5
ETOH	NO_2	0.019	0.883	1.473	0.117	1.5
	CN	0.034	0.840	1.478	0.160	1.1
	H	0.020	0.886	1.764	0.114	2.6
	Me	0.028	0.902	1.544	0.098	1.2
	OMe	0.041	0.905	1.578	0.095	1.3
	NMe_2	0.033	0.918	1.388	0.082	2.7
BUTOH	NO_2	0.055	0.930	1.350	0.070	1.9
	CN	0.050	0.913	1.581	0.087	1.6
	H	0.056	0.934	1.958	0.066	3.5
	Me	0.065	0.938	1.862	0.062	3.2
	OMe	0.084	0.948	2.027	0.084	2.2
	NMe_2	0.081	0.945	1.730	0.055	5.3
OCTOH	NO_2	0.090	0.946	1.523	0.054	1.8
	CN	0.082	0.863	2.890	0.137	4.0
	H	0.064	0.953	2.621	0.047	1.4
	Me	0.098	0.962	2.593	0.037	1.8
	OMe	0.107	0.947	2.623	0.053	1.9
	NMe_2	0.135	0.979	2.093	0.021	2.0

[a] τ_S and τ_L are short and long lifetimes (ns), f_S and f_L are fractional intensities, and χ^2 is the reduced chi-square, calculated using 0.2° and 0.004 for phase and modulation standard deviations, respectively.

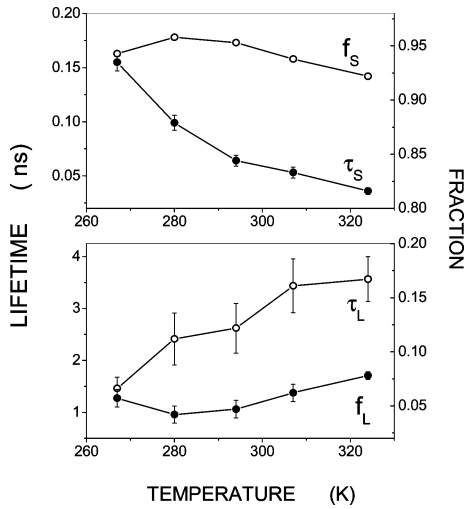

Figure 4. Lifetime and fraction of salicylideneaniline in octanol as a function of the temperature using two-exponential analysis. τ_S and τ_L are the short- and long-lifetime components, respectively.

the short lifetime and its fraction decrease in this temperature range, while the lifetime and fraction of the longer component increase. This trend is similar to that observed by increasing the aliphatic chain length of the alcohol solvent. It cannot be attributed only to the temperature effect. The viscosity of octanol changes from 25 to 4 cp when passing from 265−325 K. Therefore the trend shown in the Figure 4 must be due to both the viscosity and temperature effects.

(d) Molecular Orbital Calculation. We used the ab initio Hartree−Fock method to estimate the energy of the first excited electronic state. We have assumed that the specific solute−hydroxyl solvent interaction can be described by means of an intramolecular hydrogen bond between the solute and one methanol molecule.[17]

For compounds **1**−**6**, we have performed a full optimization of the molecular geometry in the first excited state of the keto

TABLE 3: ab initio Total Energy Calculation[a] 6-31G-CIS for the First Excited State of Enol, Keto, and Keto-Phenyl 45° Twisted

substituent	E^*_{enol} (FC)[b]	$E^*_{keto}(0°)$	$E^*_{keto}(45°)$	ΔE[e]	$\Delta E^{\#}_{ac}$[f]
NO_2[c]	−830.933826	−830.955291	−830.948465	6594 (9890)[d]	4.28
	−945.922448	−945.960555	−945.958032	8332 (10170)	1.58
CN	−719.256410	−719.288180	−719.282694	6946 (9980)	3.44
	−834.254067	−834.294360	−834.291147	8810 (11990)	2.02
H	−627.557366	−627.597847	−627.592865	8851 (10650)	3.13
	−742.561435	−742.603896	−742.600508	9285 (10450)	2.13
Me	−666.586996	−666.619115	−666.614308	7023 (9990)	3.02
	−781.584749	−781.625369	−781.621520	8881 (10170)	2.42
OMe	−741.392799	−741.422932	−741.417825	6588 (9340)	3.20
	−856.391509	−856.429628	−856.425290	8334 (9340)	2.72
NMe_2	−760.59409	−760.618413	−760.611494	5316 (7060)	4.34
	−875.593342	−875.626175	−875.618942	7179 (7250)	4.54

[a] Nonthermal ZPE correction enthalpy. [b] Optimized geometry for the fundamental state in au. [c] The first row is the solute molecule, and the second row is solute−methanol complex. [d] In parentheses are the experimental stokes shifts, in the first row in cyclohexane and second row in ethanol. [e] ΔE is the calculated Stokes shift, $\Delta E = E_{enol}^*(FC) - E_{keto}^*(0)$. Absolute values are in cm^{-1}. [f] $E^{\#}_{ac}$ is the calculated activation energy $E^{\#}_{ac} = E^*_{keto}(45) - E^*_{keto}(0)$ in kcal/mol.

TABLE 4: Global Analysis of Lifetime Data of the Salicylidenaniline in Octanol Solutions as a Function of the Temperature[a]

T, K	$(\tau_{01})^{-1}$ (ns^{-1})	k_{12} (ns^{-1})	$(\tau_{02})^{-1}$[c] (ns^{-1})	χ^2	$(\tau_S)^{-1}$ global[d] (ns^{-1})	$(\tau_S)^{-1}$[e] (ns^{-1})
264	5.85 ± 0.17[b]	0.31 ± 0.09[b]	0.44	2.5	6.15 ± 0.26	6.45
278	9.35 ± 0.35	0.82 ± 0.04	0.41	1.2	10.16 ± 0.37	10.20
294	13.69 ± 0.56	1.35 ± 0.06	0.38	1.5	15.04 ± 0.61	15.62
308	18.18 ± 0.80	1.89 ± 0.11	0.29	2.1	20.02 ± 0.94	18.88
324	23.25 ± 1.63	2.54 ± 0.38	0.27	2.5	25.79 ± 2.01	27.78

[a] $\chi^2_{global} = 2.0$, 11 free parameters, and χ^2, reduced chi-square, is calculated using 0.2° and 0.004 for phase and modulation standard deviations conditions. [b] Global error analysis. [c] Fixed parameter for biexponential analysis. [d] Calculated by $(\tau_s)^{-1} = k_{01} + k_{21}$. [e] Calculated biexponential analysis.

TABLE 5: Two Excited State Model[a]

substituent	k_{01} ns^{-1}	k_{21} ns^{-1}	k_{02} ns^{-1}	χ^2 global	$E_i^{\#}$[b] kcal	ϕ_{trans}[c]
NO_2	9.71 ± 0.42	1.49 ± 0.06	0.65	2.0	2.78 ± 0.02	0.133
CN	10.1 ± 0.36	1.34 ± 0.08	0.35	3.5	2.87 ± 0.03	0.117
H	13.2 ± 0.56	1.35 ± 0.06	0.38	2.0	2.89 ± 0.02	0.092
Me	8.70 ± 0.60	0.97 ± 0.04	0.39	4.0	3.10 ± 0.02	0.100
OMe	8.26 ± 0.37	0.80 ± 0.6	0.66	3.8	3.22 ± 0.03	0.088
NMe_2	7.14 ± 0.25	0.23 ± 0.10	0.48	2.7	4.01 ± 0.12	0.031

[a] k_{ij} is the deactivation process rate. $E_i^{\#}$ is the intrinsic molecular activation energy, and ϕ_{trans} is the efficiency of the transfer *cis*-keto* to *twist*-keto* process for the *N*-salicylidene-*p*-X-aniline compounds in octanol at 294 K. [b] $E_i^{\#}$ is calculated by eq 7 (kcal/mol), $D = 5 \times 10^{11}$ s^{-1}, $\alpha = 0.45$. [c] $\phi_{trans} = k_{21}/\{k_{01} + k_{21}\}$.

tautomer and keto-methanol. The keto-methanol is an intermolecular solute−solvent complex. The calculations reveal a coplanarity of the keto ring (K-ring) and the aniline ring (A-ring).

Table 3 displays the total energy calculated for the first singlet excited state of enol, *cis*-keto*, enol*-methanol, and *cis*-keto*-methanol complexes. For the enol structures, we have used the molecular geometry optimized for the fundamental electronic state (Franck−Condon process), and we used the total relaxed molecular geometry for the keto structures. The energy difference between these isomeric forms $\Delta E = E_{enol}^*(FC) - E_{keto}^*(0)$ corresponds to the calculated Stokes shift. These calculated values show a qualitative agreement with the experimental Stokes shift (see Table 3). This agreement is 2-fold: (a) the experimental Stokes shift increases from the cyclohexane to ethanol solution; the same happens in the calculated values, for methanol the Stokes shifts are larger than for other solvent molecules and (b) both the calculated and the experimental Stokes shifts show the same trend in the series. These two aspects allow us to validate the solute−solvent intermolecular hydrogen bond model for the description of the excited-state properties of the present compounds.

In Figure 5 we display the energy profiles, fundamental and first excited states, for the keto and keto-methanol complexes of the salicylideneaniline compound.[27,28] We have analyzed the rotations around the C_1-C_7, C_7-N, and $N-C_{1'}$ bonds. In these calculations, all the geometrical parameters were optimized at each point. For the C_1-C_7 twist (Figure 5A), in the excited state, the potential curve shows the maximum values at 45° and the minimum at 90°. Furthermore, the maximum at 90° in the fundamental electronic state produces a smaller gap between the ground and the first excited state. The rotation around the C_7-N bond is shown in Figure 5B. In the excited state, this curve shows a maximum at 60° thereby producing an estimated activation barrier of 12.4 and 5.0 kcal/mol for the keto and keto-methanol complexes, respectively. Note that there is a smooth change in the curvature in the range 75−105° which could correspond to a local minimum, not definitively identified at this level of calculation. With reference to the minimum-energy point at 0°, the curve for the keto and keto-methanol complexes display an energy difference of 11.0 and 5.0 kcal/mol, respectively. Figure 5C shows the potential energy profile for $N-C_{1'}$. In the excited state we have found only one maximum at 90°. In summary, among the three possible rotations considered here we can suggest that the most favorable is the one associated to the C_1-C_7 bond rotation.

We have also calculated the activation energy ($E^{\#}_{ac}$) for compounds **1**−**6** in the first excited state from the expression $E^{\#}_{ac} = E_{keto}^*(45) - E_{keto}^*(0)$, where $E_{keto}^*(45)$ and $E_{keto}^*(0)$ are

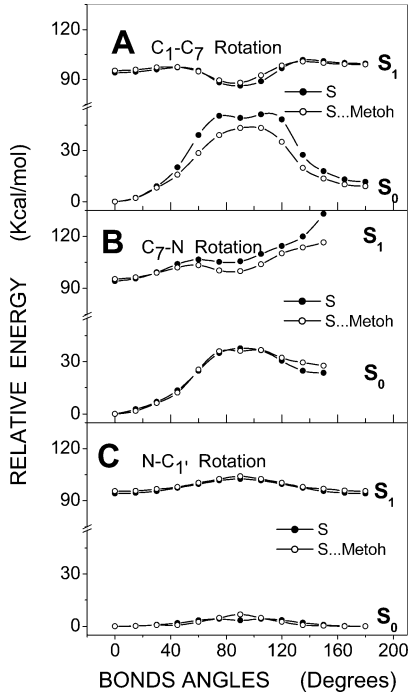

Figure 5. Ab initio HF/6-31G-CI energy profiles for the keto (●) and keto-methanol complexes (○) of the salicylideneaniline compound. S_0 and S_1 are the fundamental and first excited states, respectively.

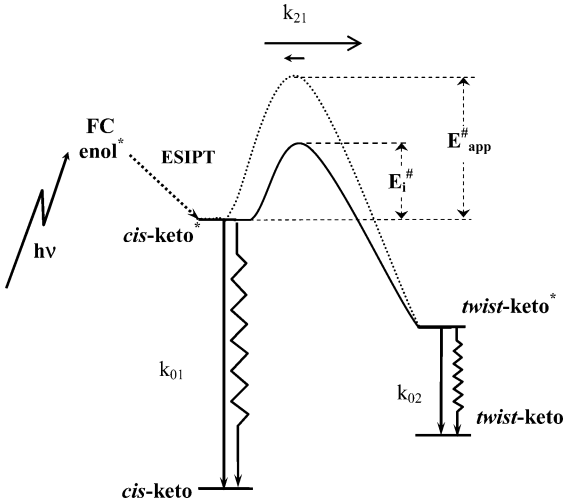

Figure 6. Two excited-state reaction kinetics scheme for *N*-salicylidene-*p*-X-aniline compounds in viscous solvent solution.

the total energies for optimized structures at 45 and 0° twist K-ring rotation angles. Calculated $E^{\#}_{ac}$ values for compounds **1**−**6** and their respective keto*-methanol complexes are shown in Table 3. The $E^{\#}_{ac}$ calculated values for the solute molecules show the largest values for the NO_2 and NMe_2 compounds, and they decrease in the nonsubstituted compound **3.** By introduction of the methanol solvent effect, which generates intermolecular hydrogen-bond complexes, we observe that $E^{\#}_{ac}$ increases with increasing the donor strength within the series.

(e) The Excited-State Deactivation Model. To explain our experimental and theoretical results, we propose a deactivation process (Figure 6) for the *N*-salicylidene-*p*-X-aniline compounds. In our model, we have considered the following previously reported information: in a rigid matrix at 77 K, the C_1-C_7, C_7-N, and $N-C_{1'}$ bond rotations are inhibited. The fluorescence increases 45−50 times with respect to that observed at 294 K.[5] Upon light absorption, the Franck−Condon excited state maintains the enol geometric structure of the fundamental state (i.e., $\theta = 45°$ and $\phi = 0°$)[17] and the intramolecular excited-state proton transfer enol* → *cis*-keto* takes place. In fluid solution (low viscosity) at 293 K after ESIPT, i.e., when the system achieves a *cis*-keto* character, the MO calculations suggest that the most probable rotation is the one involving the subunit K around the C_1-C_7 bond. Under such conditions, the fluorescence of the *cis*-keto* isomer can be quenched by internal torsion dynamic processes in the excited state. As previously suggested,[1,11−13,21] our model considers two species in the excited state, the first species, the *cis*-keto* tautomer, associated with the shortest-lifetime component and with the larger fraction, and the second species, the *twist*-keto* species associated with the longest lifetime and with the smallest fraction.

Our MO calculations show that the keto-rotated species is the C_1-C_7 bond twisted structure. (Figures 3 and 5). This species involves a twist intramolecular charge transfer state (TICT), which quenches the short lifetime component. Intrinsic molecular activation energy and solvent viscosity restrict this process.

Figure 6 shows the two excited states reaction schemes. In this figure, k_{01} and k_{02} are the deactivation rates, corresponding to transitions from the *cis*-keto* (state 1) and the *twist*-keto* (state 2) to the fundamentals *cis*-keto and *twist*-keto, respectively. The rate constant k_{21} corresponds to the *cis*-keto* to *twist*-keto* (1 → 2); k_{12} is the reverse (1 ← 2) rate constant. The τ_S and τ_L observed lifetimes shown in Table 2 are not equivalent to the time decay τ_{01} and τ_{02}, defined as the inverse of the decay rates k_{01} and k_{02}. However, τ_S and τ_L are related to the rate constant k_{ij} through eq 4

$$(\tau_S,\tau_L)^{-1} = \frac{1}{2}[\Gamma_1 + \Gamma_2 \pm [(\Gamma_1 - \Gamma_2)^2 + 4k_{21} \times k_{12}]^{1/2}] \quad (4)$$

where Γ_1 and Γ_2 given by the equations $\Gamma_1 = k_{01} + k_{21}$ and $\Gamma_2 = k_{02} + k_{12}$, are the total deactivation rates of *cis*-keto* and *twist*-keto* species, respectively. In the first excited state of salicylideneaniline compounds, the energy gap between *cis*-keto* and *twist*-keto* forms is over 10 kcal/mol, therefore, the reverse reaction rate constant k_{12} can be neglected. Under this condition, and considering eq 4, the lifetimes τ_S and τ_L are $(\tau_S)^{-1} = k_{01} + k_{21}$ and $(\tau_L)^{-1} = k_{02}$. The k_{01} and k_{21} rate constants are calculated by means of a simultaneous fit of the experimental phase and modulation data measured at five temperatures. We used the global analysis procedure with an exponential temperature link across the k_{21} rate variable.[25,26] Figure 7 displays the kinetic deactivation model fit to phase and modulation of salicylideneaniline in octanol at five temperatures. A good agreement between calculated and experimental data is obtained. The kinetic rate constants k_{ij} values are shown in Table 4. According to our model, the rate constant $(\tau_{02})^{-1}$ is fixed in the fit and it is equivalent to τ_L, which was calculated by means of discrete biexponential decay analysis. A good agreement is shown between $(\tau_S)^{-1}$ values in the last two columns of Table 4, $(\tau_S)^{-1}_{global}$ values are calculated as a sum of the rate constants $(\tau_{01})^{-1}$ and k_{21}; $(\tau_S)^{-1}_{biex}$ is obtained by a simple biexponential decay analysis. The goodness of the kinetic deactivation model is judged by the reduced global chi-square (χ_g^2) test. For this model, both the individual and the global chi squares are close to one. For the τ_{01} and k_{21} rate, we have performed a χ_g^2 error surface analysis, using the error analysis method implemented in the Global Unlimited software.[26] The results of this analysis at 294 K are shown in Figure 8. The χ_g^2 surface as a function of the τ_{01} and k_{21} parameters are approximately parabolic.

The other compounds of this series present a similar behavior

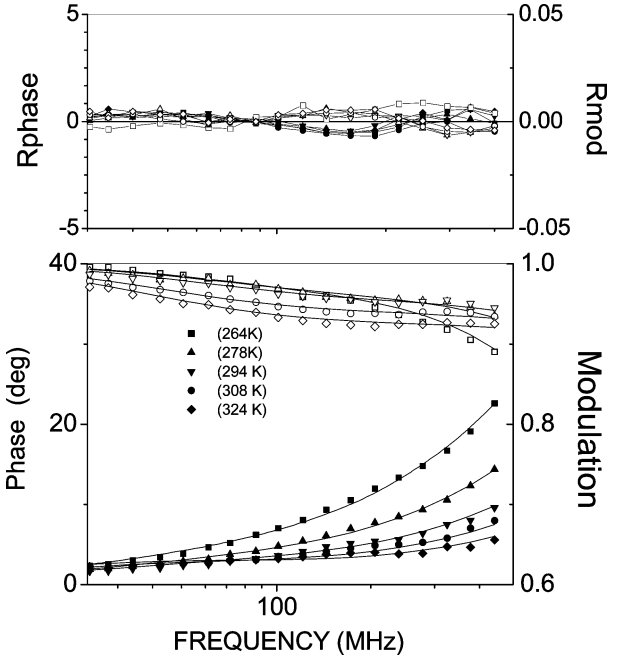

Figure 7. Global analysis fit on the salicylideneaniline compound in octanol solutions at different temperatures. Phase (filled symbols) and modulation (unfilled symbols). Solid lines correspond to the kinetic decay model.

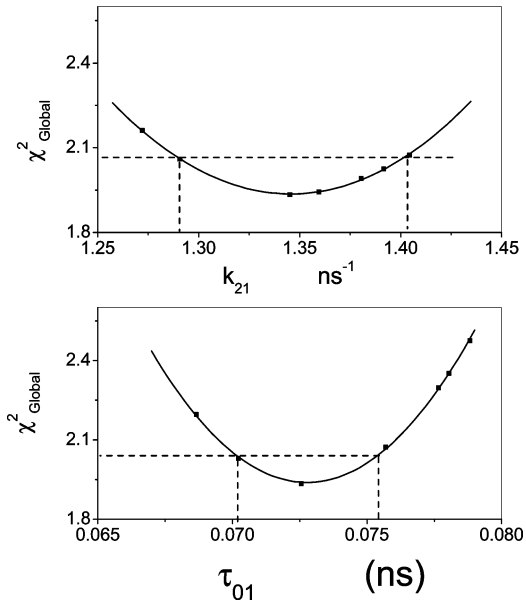

Figure 8. Chi-square global error surface for the τ_{01} and k_{21} kinetics parameters. The vertical and horizontal lines indicate the values of one standard deviation from the minimum chi-square global value.

for the salicylideneaniline compound. The kinetics rate constants k_{ij}, at 294 K for compounds **1**−**6**, are given in Table 5. The k_{21} values are related to the electronic characteristic of the substituents; they decrease as the electron-donor strength increases from NO_2 to NMe_2.

The isomerization *cis*-keto* → *twist*-keto* process depends on both the temperature and viscosity. The rate of this process $k_{21}(\eta,T)$ is well described by eq 5[29]

$$k_{21}(\eta,T) = D\eta^{-\alpha}\, e^{-E^{\#}_{i}/RT}, \text{ with } 0 < \alpha < 1 \qquad (5)$$

where D is the viscosity independent intramolecular diffusion constant and α is a measure of the strength of viscosity control;

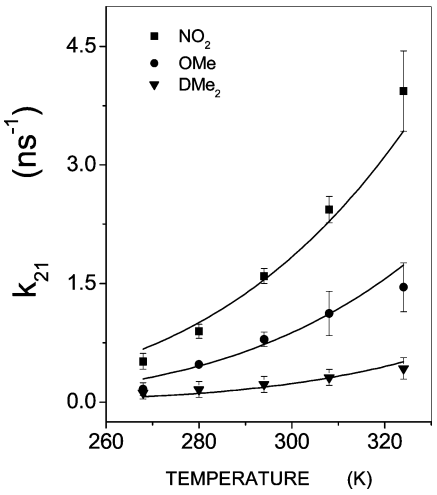

Figure 9. Global k_{21} rate constants as a function of the temperature of the NO_2, OMe, and NMe_2 in octanol. The continuous line is the fit of eq 7 to experimental data.

$E^{\#}_{i}$ is the intrinsic molecular activation energy. Considering the Andrade equation (eq 6),[30] the rate $k_{12}(\eta,T)$ can be written only in terms of the temperature variable

$$\eta(T) = \eta_{\infty}\, e^{-E^{\#}_{\eta}/RT} \qquad (6)$$

and

$$k_{21}(T) = D\eta_{\infty}^{-\alpha}\, e^{\frac{-(\alpha E^{\#}_{\eta} + E^{\#}_{i})}{RT}} \qquad (7)$$

where η_{∞} represents the viscosity of the solvent at high temperatures and $E^{\#}_{\eta}$ is the activation energy for the viscous flow of the solvent. Equation 7 has the form of the Arrhenius equations; the term $E^{\#}_{app} = \alpha E^{\#}_{\eta} + E^{\#}_{i}$ is an apparent activation barrier. We have calculated $\eta_{\infty} = 0.0019$ cp and $E^{\#}_{\eta} = 4.98 \pm 0.06$ kcal/mol for octanol. Figure 9, shows the global-calculated k_{21} rate constant as a function of the temperature for compounds **1**, **5**, and **6**. The solid line corresponds to the fitting of these experimental data to eq 7 by using $\alpha = 0.45$ and $D = 5 \times 10^{11}$ s^{-1}. $E^{\#}_{i}$ calculated values using this procedure are given in the Table 5. This energy $E^{\#}_{i}$ increases as the electron-donor strength increases from NO_2 to NMe_2. The same trend is predicted from the ab initio activation energy data.

The proposed model for the deactivation processes is consistent with the experimental data. Thus, it is possible to infer about other spectroscopy parameters such as the efficiency of the tautomeric *cis*-keto* to *twist*-keto* transfer process. The efficiency for the transfer process (ϕ_{trans}) is calculated by means of $\phi_{trans} = k_{21}/\{k_{01} + k_{21}\}$, where k_{21} and k_{01} are rate constants already defined. The ϕ_{trans} values at 294 K are displayed in Table 5. On the basis of our data and the low values of ϕ_{trans}, we establish that the isomeric *cis*-keto* form of the species under study principally deactivates via a radiative process. Furthermore, ϕ_{trans} values corroborate the dependence of the substituents effect, showing that their values decrease as the electron-donor strength of the substitution in the aniline ring increases.

Conclusions

The frequency-domain lifetime techniques have been used to determine the lifetime and rate constants describing the deactivation mechanism from the first electronic excited state of the *N*-salicylidene-*p*-X-aninile compounds.

The intermolecular hydrogen bond between *N*-salicylidene-*p*-X-aninile compounds and one molecule of methanol, characterized by means of ab initio 6-31G molecular orbital calculations (solute−methanol complex), have been shown to be an adequate model to explain the activation energy of the *cis*-keto* → *twist*-keto* process.

The two excited-state reaction models that describe the deactivation of the first electronic state of *N*-salicylidene-*p*-X-aninile compounds and the rate constant calculated by means of the global analysis procedure reveal that ϕ_{trans} values are close to 0.1. These values decrease by increasing the electron donor strength of the substituent.

Acknowledgment. The author acknowledges FONDECYT, Grant 1970787, and Universidad de Chile, DID ENL-2001-13 and Chemistry Department Grants, for financial support. Lifetime measurements were performed at the Laboratory for Fluorescence Dynamics funded by NIH-P41 RR 3155-18, Urbana, IL; gratitude is expressed to Drs. Theodore Hazlett and Susana Sanchez for providing technical assistance and the facilities for the experiments and to Dr. Enrico Gratton (LFD) for the reading of the manuscript.

References and Notes

(1) Ormsom, S. M.; Browm, R. G. *Prog. React. Kinet.* **1994**, *19*, 45.
(2) Hadjoudis, E. *Mol. Eng.* **1995**, *5*, 301.
(3) Becker, R. S.; Richey, F. *J. Am. Chem. Soc.* **1967**, *89*, 1298.
(4) Schwartz, B. J.; Peteanu, L. A.; Harris, C. B. *J. Phys. Chem.* **1992**, *96*, 3591.
(5) Antonov, L.; Fabian, W.; Nedeltcheva, D.; Kamounah, D. *J. Chem. Soc., Perkin Trans. 2* **2000**, 1173.
(6) LeGourriérec, D.; Khalanov, V.; Brown, R.; Rettig, W. *J. Photochem. Photobiol., A* **2000**, *130*, 101.
(7) Catalan, J.; Valle, J. C. *J. Am. Chem. Soc.* **1992**, *115*, 4321.
(8) Acuña, A. U.; Amat, F.; Catalán, J.; Costella, A.; Figueroa, J. M.; Muñoz, J. M. *Chem. Phys. Lett.* **1986**, *132*, 567.
(9) Sharma, K. S.; Brusham, K.; Sing, G. P. *J. Photochem. Photobiol., A* **1990**, *52*, 473.
(10) Stephan, J. S.; Moorzinki, A.; Rios-Rodriguez, C.; Grellman, K. H. *Chem. Phys. Lett.* **1994**, *229*, 541.
(11) Barbara, P. F.; Rentzepis, P. M.; Brus; L. E. *J. Am. Chem. Soc.* **1980**, *102*, 2786.
(12) Knyazhansky, M. I.; Metelitza, A. V.; Buskov, A. J.; Aldoshim, S. M. *J. Photochem. Photobiol., A* **1996**, *97*, 121.
(13) Sekikawa, T.; Kobayashi, T. *J. Phys. Chem.* **1997**, *101*, 644.
(14) Mitra, S.; Tamai, N. *Chem. Phys. Lett.* **1998**, *282*, 391.
(15) Mitra, S.; Tamai, N. *Chem. Phys.* **1999**, *246*, 463.
(16) Morales, R. G.; Jara, G. P.; Vargas, V. *Spectrosc. Lett.* **2001**, *34*, 1.
(17) Vargas, V.; Amigo, L. *J. Chem. Soc., Perkin Trans. 2* **2001**, 1124.
(18) Koll, A.; Filarowski, A.; Fitzmaurice, D.; Waghorne, E.; Mandal, A.; Mukherjee, S. *Spectrochim. Acta, Part A* **2002**, *58*, 197.
(19) Dziebowska, T.; Jagodzinska, E.; Rozwadowski, Z.; Kotfica, M. *J. Mol. Struct.* **2001**, *598*, 229.
(20) Joshi, H.; Kamounah, F. J.; Gooijer, C.; Van der Zwan, G.; Antonov, L. *J. Photochem. Photobiol., A* **2002**, *152*, 183.
(21) Kletskii, M. E.; Millov, A. A.; Metelitsa, A. V.; Knyashansky, M. I. *J. Photochem. Photobiol., A* **1997**, *110*, 267.
(22) Enchev, V.; Ugrinov, A.; Neykov, G. D. *THEOCHEM* **2000**, *530*, 223.
(23) Lee, Ho-hi; Kitagawa, T. *Bull. Chem. Soc. Jpn.* **1986**, *59*, 2897.
(24) Jameson, D. M.; Hazlett, T. *Biophysical and Biochemical Aspects of fluorescence Spectroscopy;* Dewey, T. G., Ed.; Plenum Press: 1991, pp 105−133.
(25) Gratton, E.; Limkeman, M. *Biophys. J.* **1983**, *44*, 315.
(26) Beechem, J. M.; Graton, E.; Mantulin, W. W. *Globals Unlimited Software R.3*; University of Illinois, 1990.
(27) Frisch, M. J.; Trucks, G. W.; Schlegel, H. B.; Scuseria, G. E.; Robb, M. A.; Cheeseman, J. R.; Zakrzewski, V. G.; Montgomery, J. A., Jr.; Stratmann, R. E.; Burant, J. C.; Dapprich, S.; Millam, J. M.; Daniels, A. D.; Kudin, K. N.; Strain, M. C.; Farkas, O.; Tomasi, J.; Barone, V.; Cossi, M.; Cammi, R.; Mennucci, B.; Pomelli, C.; Adamo, C.; Clifford, S.; Ochterski, J.; Petersson, G. A.; Ayala, P. Y.; Cui, Q.; Morokuma, K.; Malick, D. K.; Rabuck, A. D.; Raghavachari, K.; Foresman, J. B.; Cioslowski, J.; Ortiz, J. V.; Stefanov, B. B.; Liu, G.; Liashenko, A.; Piskorz, P.; Komaromi, I.; Gomperts, R.; Martin, R. L.; Fox, D. J.; Keith, T.; Al-Laham, M. A.; Peng, C. Y.; Nanayakkara, A.; Gonzalez, C.; Challacombe, M.; Gill, P. M. W.; Johnson, B. G.; Chen, W.; Wong, M. W.; Andres, J. L.; Head-Gordon, M.; Replogle, E. S.; Pople, J. A. *Gaussian 98*, revision A.7; Gaussian, Inc.: Pittsburgh, PA, 1998.
(28) Foresman, J. B.; Frisch, A. *Exploring Chemistry with Electronic Structure Methods*; Gaussian, Inc.: Pittsburgh, PA, 1996; Vol II.
(29) Maus, M. Photoinduced Intramolecular Charge Transfer in Donor−Acceptor Biaryls and Resulting Applicational Aspects Regarding Fluorescent Probes and Solar Energy Conversion. Ph.D. Thesis. Humboldt-Universität zu Berlin, 1998.
(30) Atkins, P. *Physical Chemistry*; W. H. Freeman and Co.: New York, 1997; Vol VI, p 736.